# Comparative study: The effects of solvent on the morphology, optical and structural features of regioregular poly(3-hexylthiophene): fullerene thin films

David E. Motaung[1, 2], Gerald F. Malgas[1,*], Christopher J. Arendse[2], and Dirk Knoesen[2]

[1]National Centre for Nano-structured Materials, Council for Scientific and Industrial Research, P. O. Box 395, Pretoria, 0001, South Africa
[2]Department of Physics, University of the Western Cape, Private Bag X17, Bellville, 7535, South Africa

## ABSTRACT

In this report the effect of solvent to control the degree of mixing of the polymer and fullerene components, as well as the domain size and charge transport properties of the blends were investigated in detail using P3HT: $C_{60}$ films. Films spin coated from a faster evaporating solvent such as an aromatic solvents demonstrate an improved ordering and a higher surface roughness in P3HT and blended films indicating that the limited solubility of P3HT:$C_{60}$ in a marginal solvent can lead directly to optimal morphologies on the films. The PL quenched by a factor of 3 after blending the P3HT with $C_{60}$ in a 1:1 wt. ratio using CB, xylene, DCB, and toluene as solvents, indicating a partially charge transfer from P3HT to $C_{60}$.

***Keywords:*** Poly-3-hexylthiophene, fullerene, polymer solar cells, morphology

[*] Corresponding Author: Dr. Gerald Malgas, Tel: (+27) 012 841 3972, Fax: (+27) 012 841 2229, Email: gmalgas@csir.co.za

# 1. INTRODUCTION

In the last decade, solution processible organic conducting and semiconducting polymers have been extensively studied for use in organic solar cells due to their low-cost synthesis, low thermal budget and direct-writing printing techniques **[1-4]**. However, various properties of conducting polymers such as the charge mobility and electrical conductivity need to be improved in order to achieve the performance level of solar cells based on its inorganic crystalline and amorphous counterparts.

Poly(3-hexylthiophene) (P3HT) is a widely used organic semiconductor and therefore it is a good candidate for application in polymer solar cells **[5]**. P3HT shows good environmental stability **[6]**, proper field-effect mobility of 0.01- 0.1 $cm^2/Vs$, reasonably high hole mobility in the range of $10^{-3}$ $cm^2$ $V^{-1}$ $s^{-1}$ **[7]**, has an absorption edge around 1.9 - 2.0 eV **[8]** and has a high solubility (solution processability). The excellent mobility of P3HT is thought to be due to the lamella-type stacking of the side chains and the stacking of thiophene rings, and thus the strong interchain interactions **[9, 10]**. In the past few years the technology of polymer photovoltaics has seen some drastic improvements in their power conversion efficiency **[11]**. Power conversion efficiencies in the 5% range have been achieved **[12,13]** by optimizing the fabrication process, such as by annealing devices in a particular range of temperatures **[13]** or in a microwave oven **[14]** for an adequate period, or by carefully controlling the solvent evaporation rate **[15]** to induce the formation of a nanoscaled bi-continuous interpenetrating network with a high interfacial area to increase exciton dissociation

efficiency and the ordered stacking structure of the polymer chains and thereby enhance the charge mobility. For achieving such a high interfacial area, the electron acceptor material must have a high solubility in the organic solvent. Therefore, fullerene derivatives should be use as the electron acceptor for homogeneous, thin film formation from solutions with optical quality **[16]**.

In spite of these recent works no unambiguous result as to the optimal processing for device performance has been established to date. In this paper the effect of solvent to control the degree of mixing of the polymer and fullerene components, as well as the domain size and charge transport properties of the blends were investigated in detail using P3HT: $C_{60}$ films with different weight ratios.

## 2. EXPERIMENT DETAILS

### *2.1 Sample preparation*

Sample preparations were done according to the following procedure. All chemicals used in this experiment were purchased from Sigma Aldrich. Regioregular poly (3-hexylthiophene) (rr-P3HT) was used as a light absorption and electron donating material; while the $C_{60}$ fullerene was used as an electron acceptor material. The molecular weight ($M_n$) of P3HT reported by Sigma Aldrich was ~64,000 $gmol^{-1}$; with regularity that is greater than 98.5 % for head-to-tail. Regioregularity denotes the percentage of stereo-regular head-to-tail (HT) attachments of the hexyl side chains to the

3-position of the thiophene rings **[17]**. These materials were used as received, without any further purification. Indium tin oxide (ITO) coated on a 1 mm glass substrate with a resistance between 8 and 12 $\Omega sq^{-1}$, and silicon (Si) (100) substrates were successfully cleaned by consecutive ultrasonication in acetone, isopropanol and de-ionized water for 10 min and dried in dry nitrogen. The active layer (i.e. the layer in which the majority of the incident light is absorbed and charges are generated) containing rr-P3HT and $C_{60}$ with different weight ratios (P3HT: $C_{60}$, e.g. 1:0, 1:1 wt. ratio) was dissolved in 1mL of non-aromatic solvents (Tetrahydrofuran (THF) and Chloroform) and aromatic solvents (Dichlorobenzene (DCB), Toluene, Xylene and Chlorobenzene (CB) solutions). The solutions were stirred overnight on a hot plate at a temperature of 50 °C to promote a complete dissolution. P3HT and its blends with a thickness of about 100 nm were spin coated onto the ITO and Si substrates. The spinning rate and time of spin-coating were 2500 rpm and 30 s. The samples were dried on a hot plate at a temperature of 50 °C for 15 min.

### *2.2 Characterization*

Atomic force microscope (AFM) (Veeco Digital Instruments Multimode), operating in the tapping mode using a phosphorus doped silicon cantilever with a spring constant of 40 $Nm^{-1}$ and a tip radius of <10 nm, was used to characterize the morphology of the P3HT and its blend. The microstructure of the P3HT and its blends was studied with a Carl Zeiss Imager Z1M polarised optical microscope (POM). Spin-coated thin films were placed between two covering glasses and placed on a Linkam hot-stage (Linkam

Scientific Instruments Ltd, UK), mounted on a POM instrument. Samples were heated from room temperature up to 250 °C at a heating rate of 10 °Cmin$^{-1}$, held at 250 °C for 1 min and then cooled down to room temperature at a precisely controlled cooling rate of 10 °Cmin$^{-1}$. The films thickness was measured using a Veeco DEKTAK 6M Stylus profilometer.

The orientation and crystallinity of the P3HT and blends films spin-coated onto Si substrates, perhaps the most significant factors enhancing P3HT thin film properties, were characterized by Panalytical X'pert PRO PW 3040/60 x-ray diffractometer with a Cu $K_\alpha$ ($\lambda$ = 0.154 nm) monochromated radiation source, operating at 45.0 kV and 40.0 mA. XRD data were collected in the $2\theta$ ranging from 3 to 25° with a step size of 0.02°. The absorption spectra of the active layer of P3HT and $C_{60}$ organic layers were measured by a PerkinElmer Ultra Violet-Visible (UV-vis) spectrometer from 900 to 300 nm. For Photoluminescence (PL), Raman and Fourier transform infrared spectroscopy (FTIR) measurements; samples were spin-coated on Si substrates. The photoluminescence (PL) spectra were taken from 300 to 900 nm by exciting the samples with 350 nm line of deuterium lamp. The emission was detected with Jobin-Yvon PMT detector. The structural properties of P3HT and its blend were investigated by PerkinElmer Fourier transform infrared spectroscopy spectrometer and Horiba Jobin Yvon HR800 micro-Raman spectrometer in backscattering geometry at room temperature. The Raman spectra were collected in the region 100–3000 cm$^{-1}$ with a spectral resolution of 0.4 cm$^{-1}$, using an excitation wavelength of 514.5 nm which was directed perpendicular to the Si substrate.

## 3. RESULTS AND DISCUSSION

### *3.1. Morphology*

Figure 1 shows the tapping-mode atomic force microscopy (AFM) images of the surface topography of as-prepared P3HT:$C_{60}$ (1:1 wt. ratio) films prepared from different solvents. The figures clearly reveal the different surface topographies between the films prepared from aromatic and non-aromatic solvents, illustrating that the surface topography is strongly dependent on the solvent used for spin-coating. The films spin-cast from non-aromatic solvents shows a high root mean square (rms) roughness ($\sigma_{rms}$) of 11.3 and 13.0 nm for chloroform and THF, respectively, where the films spin-cast from chloroform solvent (Fig. 1c) revealed nanorods, which are clearly resolved on the entire area of the scan. However, films spin-cast from the aromatic solvents exhibited a nearly smooth surface with a roughness of 0.84, 2.79, 1.71 and 4.56 nm for DCB, toluene, CB and xylene, respectively. Blend films prepared from non-aromatic solvents, which have quicker evaporation time, have a higher roughness than the films prepared from aromatic solvents.

The difference in roughness can also be attributed to the different solubility of $C_{60}$ (Table 1) in different solvents, which results in a different phase separation. Additionally, the high surface roughness in the films prepared from non-aromatic solvents is also most likely related to a signature of polymer reorganization, which in turn enhances ordered structure formation in the thin film and also increases the carrier mobility which could produce a higher efficiency from the devices. This can also be

related to the lower solubility of $C_{60}$ (Table 1), which normally forms clusters around the film and act as better pathways for charge-carrier transport in the polymer phase **[18]**.

The microstructure of the blends spin-coated on Si substrates and prepared from different solvents was studied using polarised optical microscopy (POM) technique. It is evident in Figure 2(a-c, e) that the films investigated at room temperature shows small aggregates which are related to $C_{60}$ fullerene clusters embedded in a polymer-rich skin layer, while the films prepared from CB and DCB (inset in Fig 2g) shows no aggregates associated with $C_{60}$. This is due to their high solubility of $C_{60}$ fullerene in CB and DCB. The observed $C_{60}$ clusters, especially in the case of the THF and chloroform solutions are in good agreement with the high surface roughness observed in AFM results.

To study the effect of temperature on the P3HT:$C_{60}$ (1:1 wt. ratio) films, the samples spin-cast from chloroform solvent were heated from room temperature to 250 ºC at a heating rate of 10 ºCmin$^{-1}$, dwelled at 250 °C for 1 min and then cooled down to room temperature at a precisely controlled cooling rate of 10 °Cmin$^{-1}$. It can clearly be seen in Figure 2 (e-h) as well as on the inset (Fig. 2a) that, during heating treatment, the changes in colour visible of as-prepared film is observed. The changes in colour visible during this treatment may correspond to P3HT crystallization and a depletion of $C_{60}$ which would occur between around 72 to 170 °C, followed by melting from 200 to 250 ºC. At a temperature of 250 ºC (Figure 2h), the surface of the

film became smoother and the aggregate domains, probably related to $C_{60}$ are invisible.

A similar behavior in colour change and a depletion of a soluble fullerene derivative, phenyl-$C_{61}$-butyric acid methyl ester (PCBM) around 250 ºC was also observed by Campoy-Quiles et al. **[21]**. Differential scanning calorimetry (DSC) measurements showed that, rr-P3HT exhibit an exothermic transition from a crystalline to a liquid crystalline state around 229 °C **[22]**. Chen et al. **[23]** also showed a melting temperature of 240–245 °C for head-to-tail rr-P3HT. Previous experimental POM results **[24]** showed that during annealing the P3HT films and its blend exhibit larger stains (aggregate domains). An increase in aggregates related to $C_{60}$ clusters, diffused out of the polymer matrix during annealing.

*3.2. Structural properties*

To determine the structural information (chain orientation and crystallinity) of the P3HT film and its blend, the x-ray diffraction (XRD) measurements were carried out on the films spin-coated on Si (100) substrates. Figure 3 depicts the XRD patterns of the P3HT film as well as the blend of P3HT:$C_{60}$ (1:1 wt. ratio) prepared from different solvents. The P3HT polymer prepared from non-aromatic solvents such as chloroform and THF shows well defined diffraction peaks around $2\theta$ = 5.5, 10.7 and 15.9º (Fig. 3a) and (Table 2). These well defined diffraction patterns correspond to an ordered, self-organized lamellae structure with an interlayer spacing, which is formed by parallel stacks of polymer main chains that are separated

by regions that are filled with the alkyl side-chains **[23, 25-29]**. The films spin-cast from DCB and CB solvents showed only the (100) diffraction patterns.

When P3HT polymer is blended with $C_{60}$ fullerene (Fig. 3b), the P3HT diffraction peaks for (100), (200) and (300), as well as the (220), (311), (222) and (331) diffraction peaks at 17.7, 20.9 and 21.7° associated with $C_{60}$ were only observed on the films spin cast from THF and chloroform, respectively **[30]**. The observed diffraction peaks for blend films spin-cast from chloroform and THF solutions illustrate that the P3HT material still maintains its structure and it is not hindered by the addition of $C_{60}$, due to their low boiling point (Table 1) which offers an advantage of fast solvent drying time to deposit highly crystalline P3HT film **[31]**.

The low intensity (lower crystallinity) peaks observed for blends spin-coated from aromatic solvents, such as Toluene, DCB and CB, indicates that P3HT crystallization is hindered and disordered with an addition of $C_{60}$ fullerene. However, Kline et al. **[32]** found that P3HT films cast in xylene have substantially higher crystallinity than their chloroform counterparts. Considering, the above results (Fig. 3), it can be suggested that, the faster evaporation time and limited solubility of rr-P3HT and $C_{60}$ in both solvents (chloroform and THF solution) for spin-casting offers rr-P3HT and its blend to form a more kinetically favourable crystal structure and crystallization **[31]**, where hexyl side chains of rr-P3HT are oriented parallel to the substrate, i.e., vertically $\pi$-$\pi$ stacking of inter-rr P3HTs on the substrate

(inset in Fig. 3a). In addition, it can also be inferred that in the non-aromatic solvents the beam is more highly scattered due the substantial ordering of the polymer as well by $C_{60}$ clusters formation induced by lower solubility solvents in $C_{60}$. However, in the films spin-cast in aromatic solvents the scattered beam experiences a smooth interface between P3HT and $C_{60}$ induced by high solubility of $C_{60}$ in aromatic solvents (Table 1).

Using Bragg's equation **[28, 29, 33, 34]**, the d-spacing for the primary (100) peak of P3HT and its blend was found to be between 1.55 and 1.65 ± 0.03 nm as shown in Table 2. Thus, comparing these values with the data from the literature **[25, 33-38]**, it can be concluded, that the detected peak originates from polymer crystallites with *a*-axis orientation (backbone parallel and side-chains perpendicular to the substrate, as depicted in the inset in Figure 3(a). The domain size along the *b* and *c* axes **[28]** could not be estimated from our measurements. Furthermore, using Scherrer's equation **[33, 34]** with the full width at half maximum (FWHM) of the (100) diffraction peak of the P3HT film revealed that the crystallite sizes of P3HT and blend films ranges between 9.0 and 15.0 ± 0.03 nm as presented in Table 2. An increase in crystal sizes (reduction in FWHM) was observed for the P3HT prepared from non-aromatic solvents. This indicates an increase in the ordering of the alkyl chains within the main thiophene chains. It was previously observed, using high resolution transmission electron microscopy (HR-TEM) as well as XRD, that that the structure of rr-P3HT films consists of crystallites embedded in an amorphous polymer matrix **[22, 32, 39]**.

To complement XRD, Raman spectroscopy measurements were performed on spin-coated P3HT and P3HT: $C_{60}$ (1:1 wt. ratio) films. Figure

4 present the Raman spectra of the P3HT and its blend (1:1 wt. ratio) film prepared from different solvents. In the spectrum of P3HT (Fig. 4) intensive Raman bands at about 715 , 1380 and 1440 $cm^{-1}$ are observed and are assigned to the C–S–C ring deformation, C–C skeletal stretching and C=C ring stretching, respectively **[40-42]**. However, no Raman features attributable to $C_{60}$, such as the $A_{1g}$ 1469 $cm^{-1}$ mode of fullerenes, could be resolved.

To investigate the effect of solvents on the structural properties of P3HT, we compare the 1350-1500 $cm^{-1}$ region for non-aromatic and aromatic solvents. A Lorentzian function was carried out on the Raman spectra around 1445 $cm^{-1}$ and the data are summarized in Table 3. For rr-P3HT films prepared from non-aromatic solvents (Fig. 4a), an increase on the intensity of C=C ring stretching bands is observed, indicating an ordering in the polymer. However, when P3HT is blended with $C_{60}$ fullerene (Fig. 4b), significant changes on the C=C stretching deformation is observed. The peak position shifts to higher wavenumbers ($cm^{-1}$) and the FWHM also increased with the addition of $C_{60}$. A downward shift in the wavenumber generally indicates an increase in the crystallinity of P3HT polymer and the extension of the effective conjugation length along the polymer backbone **[43]**. Similar results were also observed by Malgas et al. **[44]**.

Figure 5 presents Fourier transform infrared spectroscopy (FTIR) absorbance spectra of P3HT and blended films measured in the range of 4000–400 $cm^{-1}$. The absorption band at 3054 $cm^{-1}$ is assigned to aromatic CH stretching. This band is only observed for the P3HT films prepared from

chloroform, indicating better ordering on the polymer structure. However, for the P3HT:$C_{60}$ (1:1 wt. ratio) film (Fig. 5b), this band disappears, which is probably due to the addition of the $C_{60}$ fullerene. The bands around 2921, 2935 and 2854 $cm^{-1}$ are assigned to aliphatic CH stretching; while the bands at 1460 and 1510 $cm^{-1}$ are associated with symmetric and asymmetric ring stretching vibrations, respectively. The relative intensity ratio of the 1510 $cm^{-1}$ band to the 1460 $cm^{-1}$ band ($I_{1508}/I_{1460}$) provides information on the P3HT the conjugation length **[45, 46]**. In brief, conjugation length is the length of a completely undisturbed alternating single bond / double bond segment, being planar and allowing maximum overlap of $\pi$-electrons. In the present case for as-prepared P3HT prepared from different solvents, the $I_{1508}/I_{1460}$ ratios ranges between 0.25 and 2.0.

The absorption bands at 1377, 819 and 725 $cm^{-1}$ corresponds to the methyl deformation, aromatic C-H out-of plane and to the methyl rocking. The band at 1045 $cm^{-1}$ are assigned to $C=S^{+}\text{-}0^{-}$ residues **[47]**. The films prepared from chloroform and THF as depicted in the inset (Fig. 5) shows enhanced intensity on the aromatic C-H out-of plane and this band can be used to study the charge-transfer effect in P3HT. However, no significant changes, such as shifting of the peaks were observed on the bands. A new band appears (inset Fig. 5a) at 798 $cm^{-1}$ and disappears for the blended films. Gustafsson *et al.* **[48]** observed two peaks (at 2480 and 774 $cm^{-1}$) for fully $FeCl_3$ doped P3HT and assigned them to the formation of bi-polarons.

Therefore, we can conclude that, higher surface roughness, the presence of nanorod structures (Fig. 1), and an increase on the intensity of C=C ring stretching bands (Fig. 4) provide evidence of the better ordering of the polymer matrix in the fast drying solvents, which confirm the enhanced crystallinity observed in the corresponding XRD spectra (Fig. 3).

### *3.3. Optical properties*

Figure 6 depicts the UV-vis absorption spectra of the rr-P3HT film and its blend of P3HT:$C_{60}$ (1:1 wt. ratio) prepared from different solvents. It is evident from Figure 6(a) that the films spin-coated in non-aromatic solvents have higher absorption intensity than the aromatic solvents. This indicates that the degree of the P3HT chain ordering intra-chain interactions is higher in the case of using non-aromatic solvents **[35, 49, 50]** and is in agreement with observations made from the structural analysis. The absorption maxima are observed at the wavelengths of between 522 and 560 nm, for the film prepared from aromatic solvents. However, for non-aromatic solvents, the absorption maxima were observed around 518 and 556 nm, respectively. These bands can be ascribed to the π-π* transition **[23]**. The development of vibronic structures (i.e. the strong shoulders peaks) is also observed around 604 nm.

When P3HT is blended with $C_{60}$ (1:1 wt. ratio) as shown in Figure 6(b), an interesting effect was observed. The reduction in maximum absorption intensity and shifting in the wavelength was observed. This reduction in intensities and the shift might originate from a tighter chain coil, produced by twisting of the polymer backbone or broken conjugation in the presence of

$C_{60}$, resulting in segments with a shorter conjugation length and weaker interchain interaction. This result can also be explained by a change in the stacking conformation of the polymer structure from high crystallinity to lower crystallinity, and a reduction of intraplane and interplane stacking, which causes a poor π-π* transition and lower absorbance. This reduction in intensities was also observed in the literature **[51, 52]**.

Photoluminescence quenching in a bulk heterojunction (BHJ) is a useful indication of the degree of success of exciton dissociation. Figure 7 shows the PL spectra of P3HT and P3HT:$C_{60}$ (1:1 wt. ratio) films spin-coated from different solvents. It is apparent in Figure 7(a) that the films spin-coated from chloroform as well as in xylene solvent exhibit a reduced PL intensity. Upon introducing a $C_{60}$ fullerene as an acceptor material in the P3HT films (Fig. 7b) the PL is quenched by a factor of 3. It is also observed that the chloroform prepared film exhibits a red-shift, showing its maximum at 700 nm and a shoulder at 718 nm. The red-shift and the reduction in the PL intensity in the case of chloroform is probably due to less coarse phase separation, which promote the $C_{60}$ to be in close enough contact with the polymer to undergo a charge transfer.

Films spin-coated in other solvents, such as CB, xylene, DCB, and toluene solvents; reveal a higher PL intensity (incomplete quenching), showing that not all the excitons generated on one polymer within the film reached an interface with the other polymer. This is probably due to their higher solubility of the $C_{60}$ fullerene (Table 1) thereby inducing a finer phase separation and smaller grain size observed. Koeppe et al. **[53]** reported

that, in a finer phase separation, the photogenerated charge carriers overcome much more interfaces during their travel in a fine mixture. Therefore, it can be concluded that, the formation of inter-chain exciton and its easy dissipation to a long distance overcomes over exciton dissociation **[54]**, as chain planarity/crystallinity (Fig. 3) increases and causes decrease in PL intensity. The PL quenching observed here is suggested to be a case of self-quenching, where plainer chains allow easy going/dissipation for excitons to a long distance (10-20nm). This will allow excitons to lose their energy and lessen the probability of radiative decay.

## 4. CONCLUSION

We have studied the effect of solvents on the phase separation, crystallization and interchain interaction of P3HT and $C_{60}$ fullerene films using AFM, XRD, UV-vis, PL, Raman and FTIR spectroscopy. A high surface roughness and degree of ordering on the polymer chain were observed. This indicates that the limited solubility of rr P3HT in a marginal solvent such as non-aromatic solvents can offer a strategy to obtain highly ordered crystal structures. A red-shift and a complete reduction (quenching) in the PL intensity as well as nanorod structure were observed in the films spin-cast from chloroform. The PL quenched by a factor of 3 after blending the P3HT with $C_{60}$ in a 1:1 wt. ratio using CB, xylene, DCB, and toluene as solvents, indicating a partially charge transfer from P3HT to $C_{60}$.

## 5. AKNOWLWDGEMENTS

The authors would like to thank the financial support of the Department of Science and Technology of South Africa and the Council for Scientific Industrial Research (CSIR), South Africa (Project No. HGERA7S). The authors are also thankful to Jayita Bandyopadhyay and Thomas Malelwa (National Centre for Nano-Structured Materials, CSIR) for their valued assistance with the optical microscopy and AFM analysis.

## 6. REFERENCES


[1] C. W, Tang, Appl. Phys. Lett. 48 (1986) 183.

[2] S. E. Shaheen, R. Radspinner, N. Peyghambarian, G. E. Jabbour, Appl. Phys. Lett. 79 (2001) 2996

[3] F.C. Krebs, J. Alstrup, H. Spangaard, K. Larsen, E. Kold, Sol. Energ. Mater. Sol. Cells 83 (2004) 293

[4] T. Aernouts, in: 19th European Photovoltaics Conference, 7–11 June 2004, Paris, France.

[5] J. Y. Seong, K. S. Chung, S. K. Kwak, Y. H. Kim, D. G. Moon, J. I. Han and W. K. Kim, J. Korean Phys. Soc. 45, (2004) 5914.

[6] H. Sirringhaus, N. Tessler, R. H. Friend Science 280 (1998) 1741.

[7] S. S. Pandey, W. Takashima, S. Nagamatsu, T. Endo, M. Rikukawa, K. Kaneto, Japan. J. Appl. Phys. 39 (2000) 94.

[8] D. H. Kim, Y. D. Park, Y. S. Jang, H. C. Yang, Y. H. Kim, J. I. Han, D. G. Moon, S. J. Park, T. Y. Chang, C. W. Chang, M. K. Joo, C. Y. Ryu, K. W. Cho, Adv. Func. Mat. 15 (2005) 77.

[9] H. Sirringhaus, P. J. Brown, R. H. Friend, M. M. Nielsen, K. Bechgaard, B. M. W. Langeveld-Voss, A. J. H. Spiering, R. A. J. Janssen, E. W. Meijer, P. Herwig and D. M. de Leeuw, Nature 401 (1999) 685.

[10] X. Jiang, R. Osterbacka, O. Korovyanko, C. P. An, B. Horowitz, R. A. J. Janssen and Z. V. Vardeny, Adv. Funct. Mater. 12 (2002) 587.

[11] Special Issue: Organic-Based Photovoltaics, MRS Bull. 30 (2005) issue 1.

[12] G. Li, V. Shrotriya, J. Huang, Y. Yao, T. Moriarty, K. Emery, Y. Yang, Nature Mater. 4 (2005) 864.

[13] W. Ma, C.Y. Yang, X. Gong, K. Lee, A.J. Heeger, Adv. Funct. Mater. 15 (2005) 1617.

[14] C. J. Ko, Y. K. Lin, F. C. Chen, Adv. Mater. 19 (2007) 3520.

[15] G. Li, V. Shrotriya, J. Huang, Y. Yao, T. Moriarty, K. Emery, Y. Yang, Nature Mater. 4 (2005) 864.

[16] G. Yu, J. Gao, J. C. Hummelen, F. Wudl, A. J. Heeger, Science 270 (1665) 1789.

[17] R. D. McCullough, Adv. Mater. 10 (1998) 93.

[18] Mao-Yuan Chiu, U-Ser Jeng, Chiu-Hun Su, Keng S. Liang, and Kung Hwa Wei, Adv. Mater. 20 (2008) 2573.

[19] R. S Ruoff, D. S Tse, R. Malhotra, D. C. Lorents, J. Phys. Chem. 97 (1993) 3379.

[20] D. R. Lide, CRC Handbook of Chemistry and Physics, 82nd Ed., CRC Press, 06/2001.

[21] M. Campoy-Quiles, T. Ferenczi, T. Agostinelli, P. G. Etchegoin, Y. Kim, T. D. Anthopoulos, P. N. Stavrinou, D. D. C. Bradley, J. Nelson, Nature Mater 7 (2008)158.

[22] D. E. Motaung, et al. Sol. Energy Mater. Sol. Cells (2009), doi:10.1016/j.solmat.2009.05.016.

[23] T-A. Chen, X. Wu and D. Rieke J. Amer. Chem. Soc. 117 (1995) 233.

[24] D. E. Motaung, G. F. Malgas, C. J. Arendse S. E. Mavundla, C. J. Oliphant, D. Knoesen, J. Mater. Sci. 44 (2009) 3192.

[25] W. R. Salaneck, O. Inganas, B. Themans, J. O. Nilsson, B. Siogren, J-E. Osterholm, J-L. Bredas and S. Svensson, J. Chem. Phys. 89 (1988) 4613.

[26] P. Vanlaeke, G. Vanhoyland, T. Aernouts, D. Cheyns, C. Deibel, J. Manca, P. Heremans, J. Poortmans, Thin Solid Films 511–512 (2006) 358.

[27] P. Vanlaeke, A. Swinnen, I. Haeldermans, G. Vanhoyland, T. Aernouts, D. Cheyns, C. Deibel, J. D'Haen, P. Heremans, J. Poortmans, J.V. Manca, Sol. Energy Mater. Sol. Cells 90 (2006) 2150.

[28] T. Erb, U. Zhokhavets, G. Gobsch, S. Raleva, B. Stühn, P. Schilinsky, C. Waldauf, C.J. Brabec, Adv. Funct. Mater. 15 (2005) 1193.

[29] U. Zhokhavets, T. Erb, H. Hoppe, G. Gobsch, N.S. Sariciftci, Thin Solid Films. 496 (2006) 679.

[30] International Centre for Diffraction Data (ICDD): P3HT (48-2040), $C_{60}$ fullerene (47-0787, 44-0558).

[31] D. M. DeLongchamp, B. M. Vogel, Y. Jung, M. C. Gurau, C. A. Richter, O. A. Kirillov, J. Obrzut, D. A. Fischer, S. Sambasivan, L. J. Richter, and E. K. Lin, Chem. Mater. 17 (2005) 5610.

[32] R. J. Kline, M.D. McGehee, E.N. Kadnikova, J.S. Liu, J.M.J. Fréchet, M.F. Toney, Macromolecules 38 (2005) 3312.

[33] T. Erb, U. Zhokhavets, H. Hoppe, G. Gobsch, M. Al-Ibrahim, O. Ambacher, Thin Solid Films 511 (2006) 483.

[34] B. E Warren, X-Ray Diffraction (New York: Dover) p. 251 (1990).

[35] Y. Kim, S. Cook, S.M. Tuladhar, S.A. Choulis, J. Nelson, J.R. Durrant, D. D. C. Bradley, M. Giles, I. McCulloch, C.S. Ha, M. Ree, Nat. Mater. 5 (2006) 197.

[36] T. J. Prosa, M.J. Winokur, Macromolecules 25 (1992) 4364.

[37] K. E. Aasmundtveit, E.J. Samuelsen, M. Guldstein, C. Steinsland, O. Flornes, C. Fagermo, T.M. Seeberg, L.A.A. Pettersson, O. Ingana¨s, R. Feidenhans'l, S. Ferrer, Macromolecules 33 (2000) 3120.

[38] T. Erb, S. Raleva, U. Zhokhavets, G. Gobsch, B. Stuhn, M. Spode, O. Ambacher, Thin Solid Films 450 (2004) 97.

[39] A. Zen, J. Pflaum, S. Hirschmann, W. Zhuang, F. Jaiser, U. Asawapirom, J.P. Rabe, U. Scherf, D. Neher, Adv. Funct. Mater. 14 (2004) 757.

[40] M Baibarac, M Lapkowski, A. Pron, S. Lefrant, I. Baltog, J. Raman Spectrosc. 29 (1998) 825.

[41] P.J. Brown, D.S. Thomas, A. Kőhler, J.S. Wilson, J.-S. Kim, C.M. Ramsdale, H. Sirringhaus, R.H. Friend, Phys. Rev., B 67 (2003) 064203.

[42] G. Louarn, M. Trznadel, J.P. Buisson, J. Laska, A. Pron,M. Lapkowski, S.J. Lefrant, Phys. Chem. 100 (1996) 12532.

[43] C. Heller, G. Leising, G. Godon, S. Lefrant, W. Fischer, F. Stelzer, Phys. Rev., B 51 (1995) 8107.

[44] G. F. Malgas, C. J. Arendse, S. E. Mavundla, F. R. Cummings, J. Mater. Sci. 43 (2008) 5599.

[45] Y. Furukawa, M. Akimoto, I. Harada, Synthetic Metals 18 (1987) 151.

[46] S.S. Pandey,W. Takashima, S. Nagamatsu, K. Kaneto, IEICE Trans. Electron.,E83-C (2000) 1088.

[47] M. S.A. Abdou, S. Holdcroft, Can. J. Chem. 73 (1995) 1893.

[48] G. Gustafsson, O. Ingan¨as, J.O. Nilsson, B. Lieberg, Synth. Met. 26 (1988) 297.

[49] X. Jiang, R. Osterbacka, O. Korovyanko, C. P. An, B. Horowitz, R. A. J. Janssen and Z. V. Vardeny, Adv. Funct. Mater. 12 (2002) 587.

[50] P.J. Brown, D.S. Thomas, A. Ko¨ hler, J.S. Wilson, J.S. Kim, C.M. Ramsdale, H. Sirringhaus, R.H. Friend, Phys. Rev. B 67 (2003) 064203.

[51] V. Shrotriya, J. Ouyang, R. J. Tseng, G. Li, Y. Yang, Chemical Physics Letters 411 (2005) 138.

[52] D. Valentin, Mihailetchi, Hangxing Xie, Bert de Boer, L. Jan Anton Koster, and P. W. M. Blom, Adv. Funct. Mater. 16 (2006) 699.

[53] R. Koeppe and N. S. Sariciftci, Photochem. Photobiol. Sci. 5 (2006) 1122.

[54] M. P. Jeffrey, D. S. Richard, W. Donald. J Am Chem Soc 126(38) (2004) 11752.

Figure 1: D. E. Motaung *et..al.*

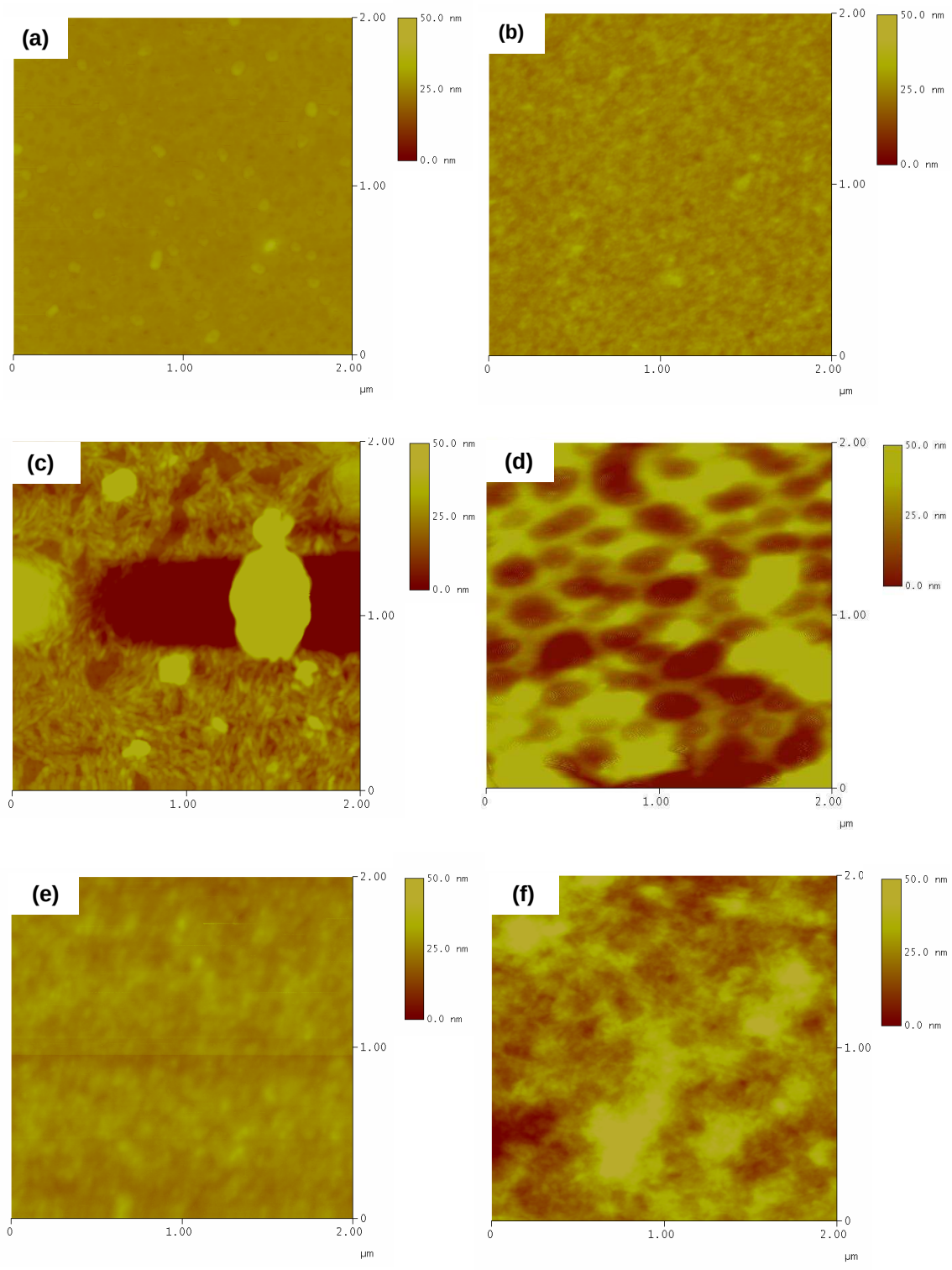

Figure 2: D. E. Motaung *et..al.*

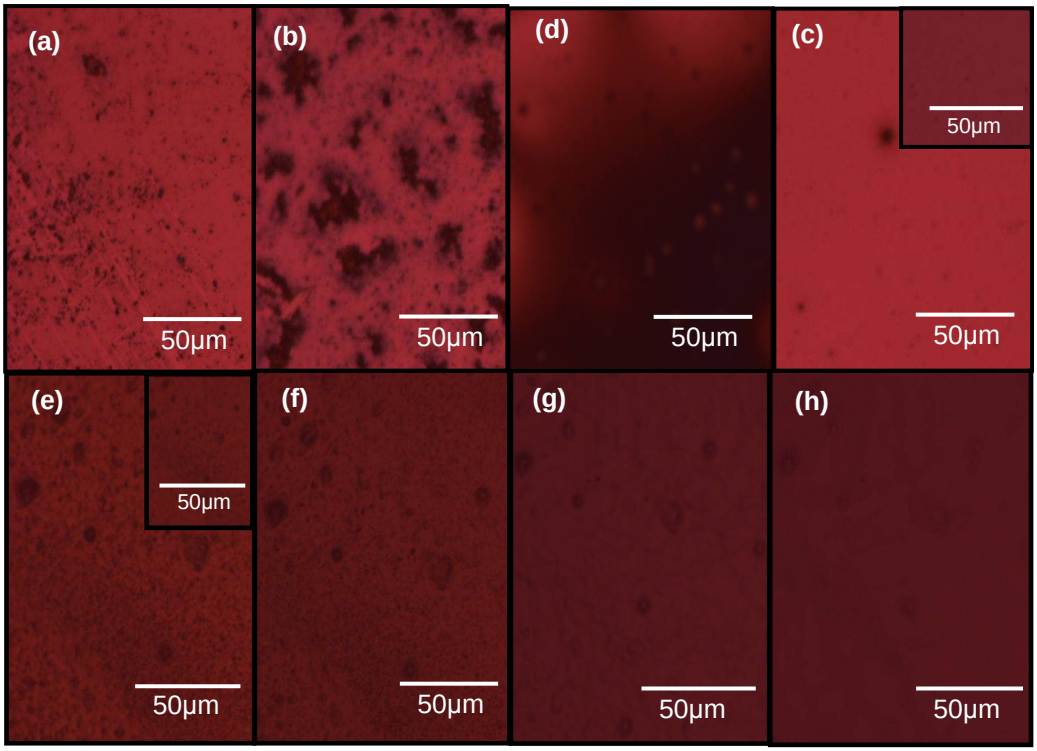

Figure 3: D. E. Motaung *et..al.*

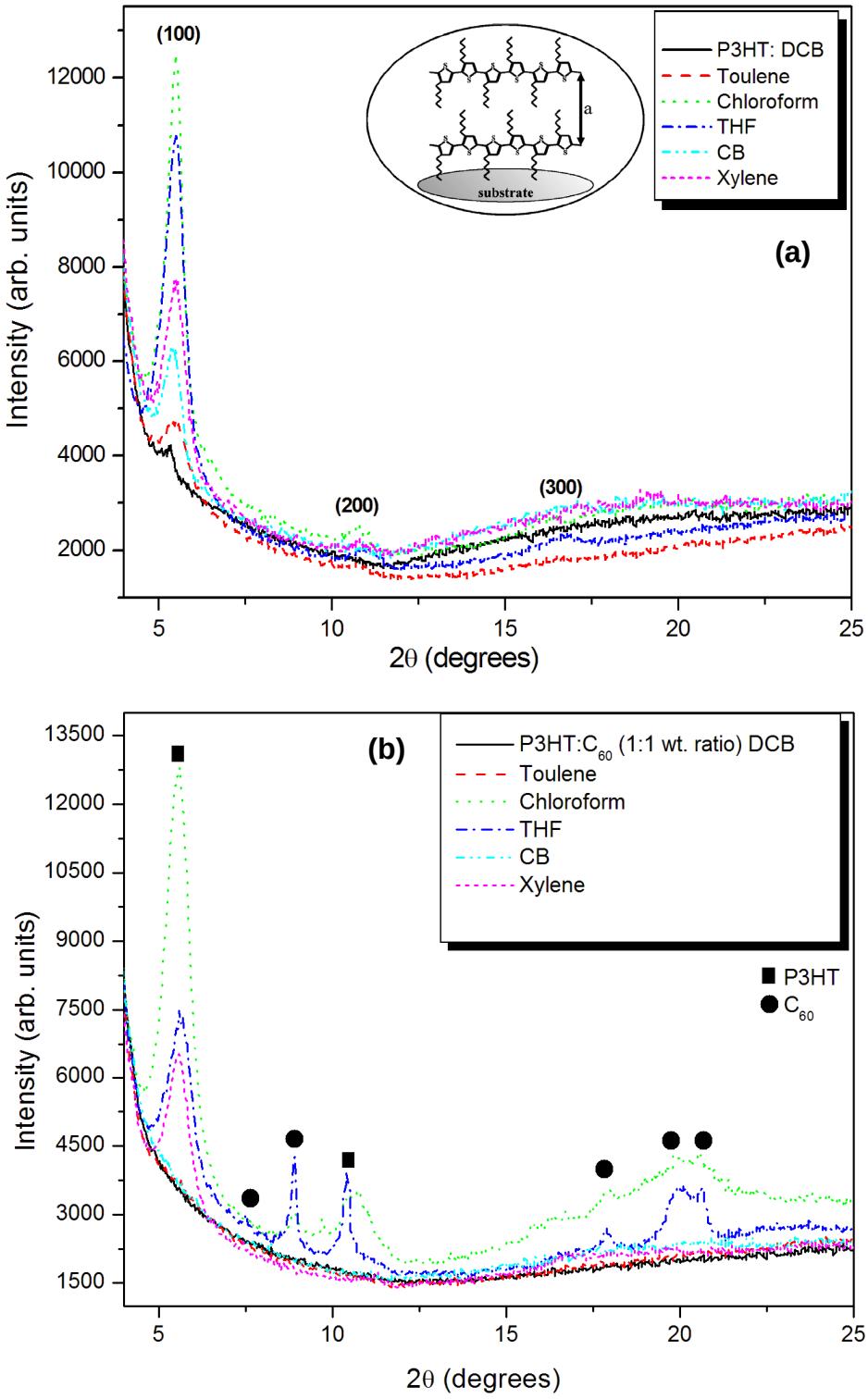

Figure 4: D. E. Motaung *et..al.*

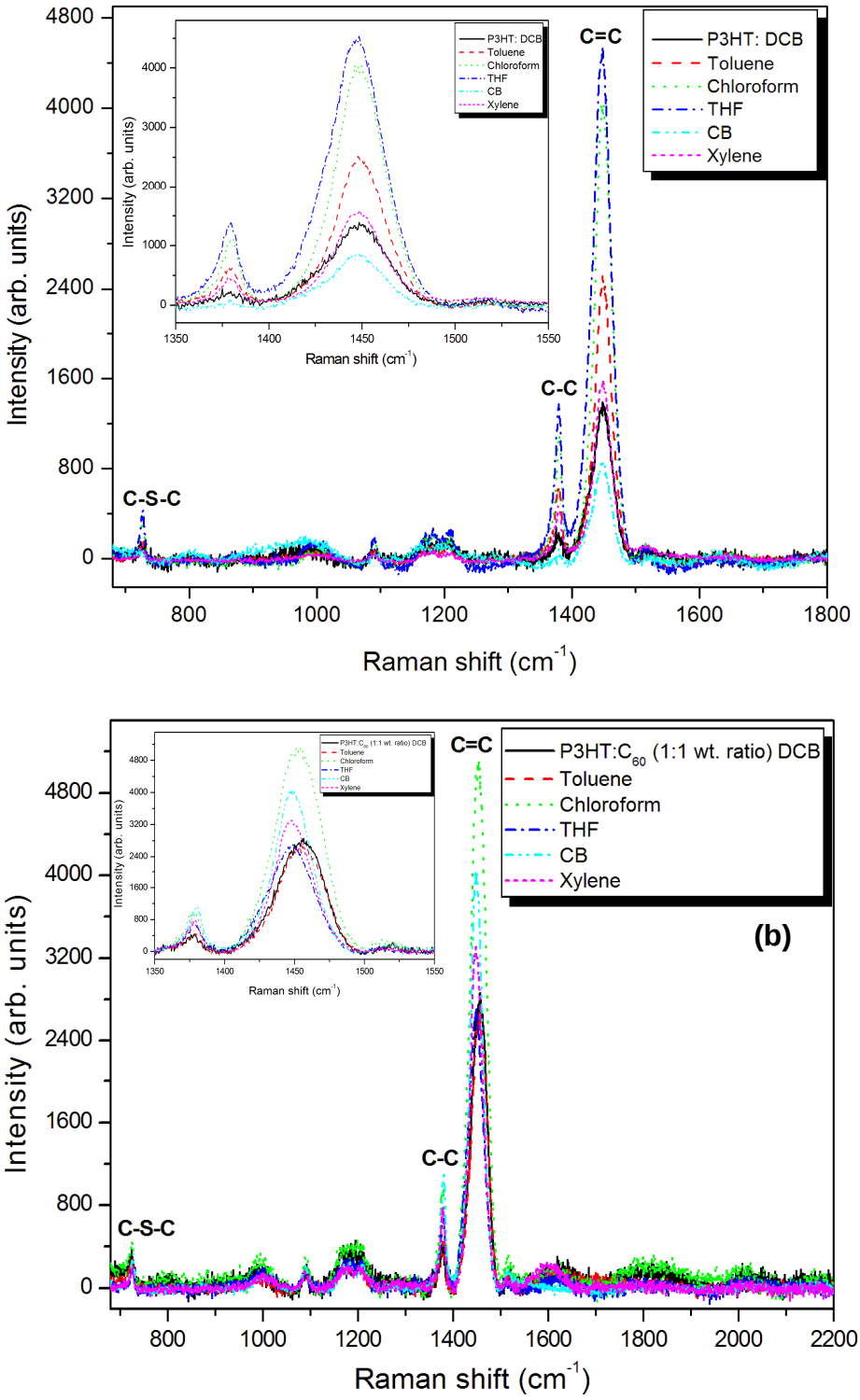

Figure 5: D. E. Motaung *et..al.*

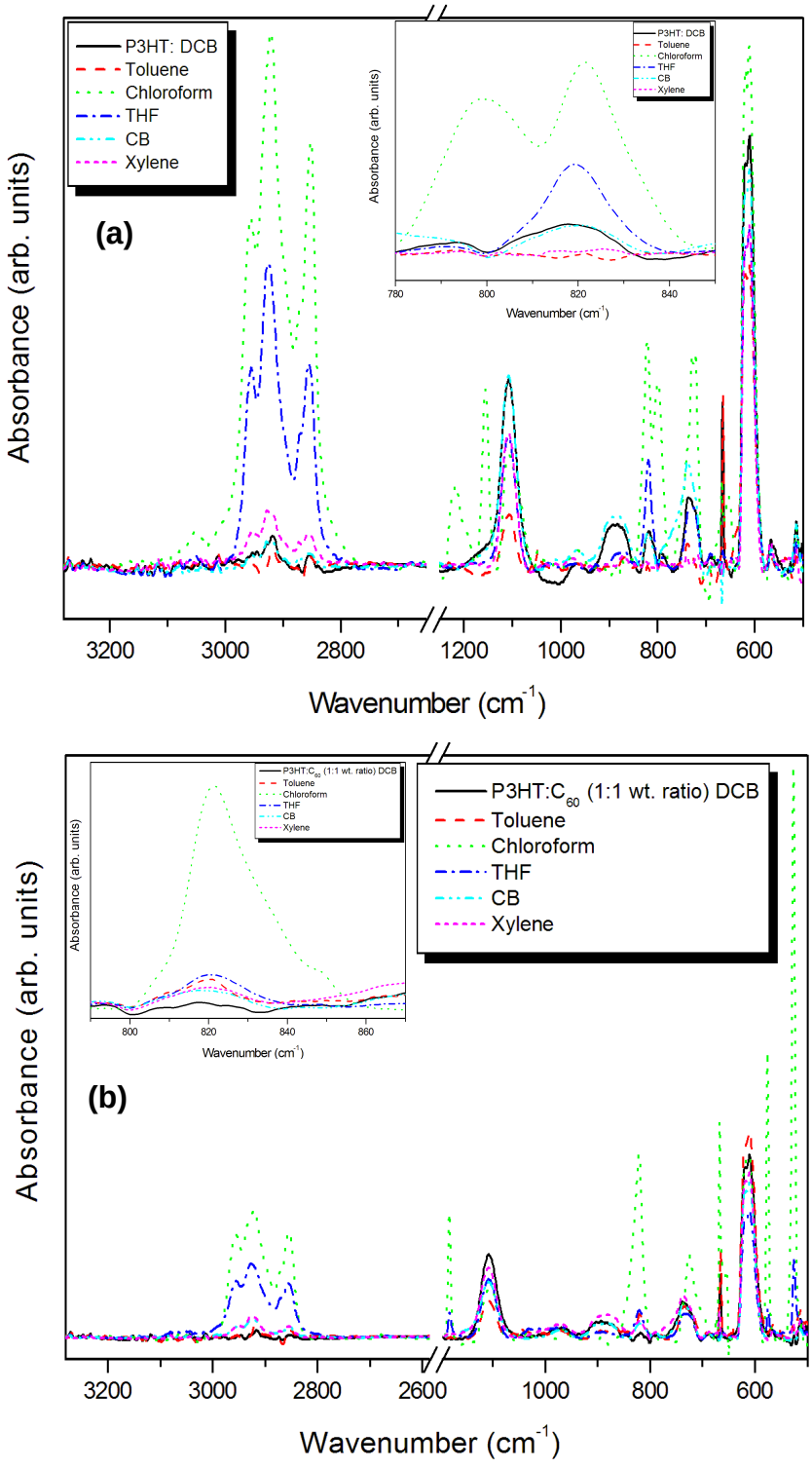

Figure 6: D. E. Motaung *et..al.*

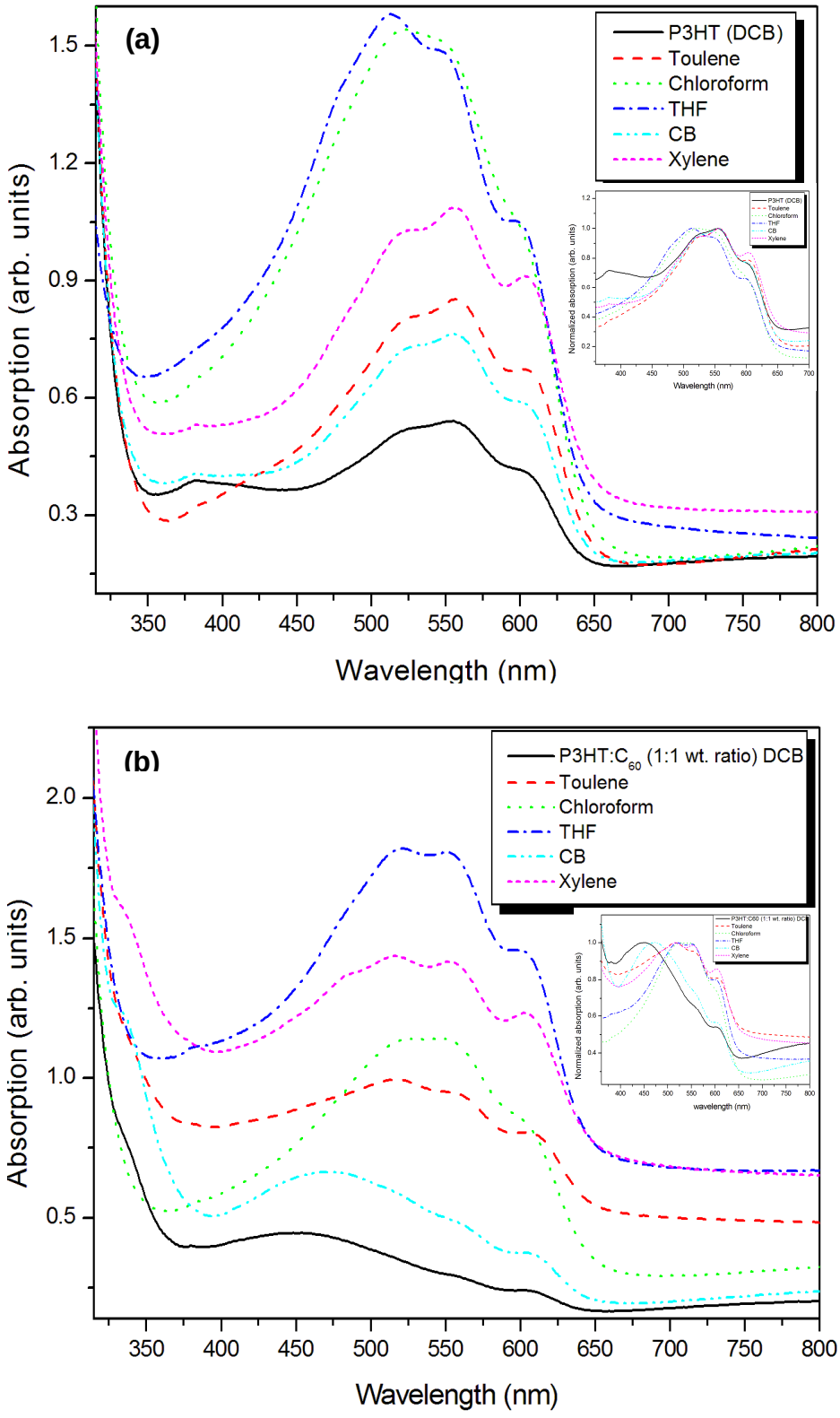

Figure 7: D. E. Motaung *et..al.*

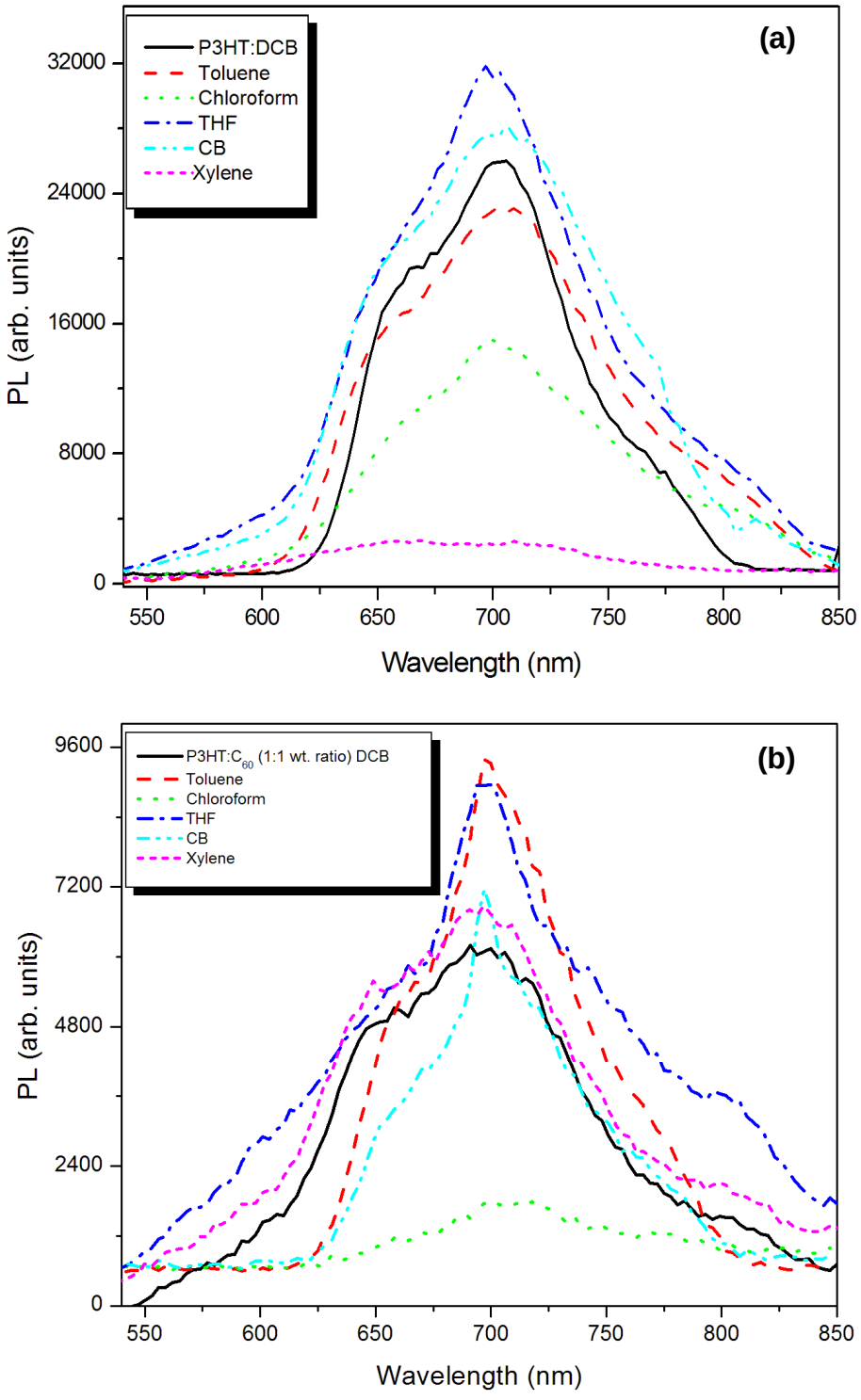

TABLE 1: D. E. Motaung *et..al.*

| Solvents | Boiling points (ºC) | $C_{60}$ Solubility (mg $mL^{-1}$) |
|---|---|---|
| Dichlorobenzene (DCB) | 180.3 | 27.0 |
| Chlorobenzene (CB) | 111.0 | 7.0 |
| Xylene | 62.0 | 5.2 |
| Toluene | 66.0 | 2.8 |
| Chloroform | 132.0 | 0.16 |
| THF | 144.0 | 0.006 |

TABLE 2: D. E. Motaung *et..al.*

| Solvents | Peak height (cts) | d-spacing (nm) | FWHM (°) | Grain size (nm) |
|---|---|---|---|---|
| DCB | 1380.64 | 1.65 | 0.82 | 9.7 |
| Toluene | 2109.29 | 1.59 | 0.77 | 10.3 |
| Chloroform | 8853.56 | 1.59 | 0.56 | 14.2 |
| THF | 8108.1 | 1.55 | 0.60 | 13.3 |
| CB | 3384.48 | 1.61 | 0.65 | 12.2 |
| Xylene | 4707.01 | 1.59 | 0.71 | 11.2 |

| Solvents | P3HT film | | | P3HT: $C_{60}$ (1:1 wt. ratio) film | | |
|---|---|---|---|---|---|---|
| | Peak position ($cm^{-1}$) | FWHM ($cm^{-1}$) | Intensity (a. u) | Peak position ($cm^{-1}$) | FWHM ($cm^{-1}$) | Intensity (a. u) |
| DCB | 1447.7 | 31.035 | 1401.8 | 1454.2 | 46.366 | 3599.3 |
| Toluene | 1449.0 | 33.986 | 2878.0 | 1454.8 | 44.399 | 3313.0 |
| Chloroform | 1448.7 | 33.993 | 4682.2 | 1452.5 | 47.708 | 6579.9 |
| THF | 1447.5 | 38.859 | 5174.2 | 1449.4 | 44.337 | 3280.3 |
| CB | 1447.6 | 38.307 | 1005.6 | 1448.9 | 34.530 | 4634.2 |
| Xylene | 1448.2 | 32.508 | 1724.0 | 1448.8 | 36.234 | 3930.8 |

**List of Tables and Figure captions**

**Figure 1:** Tapping-mode AFM topography scans (2μm×2μm) of as-prepared P3HT:$C_{60}$ (1:1 wt. ratio) films prepared from different solvents **(a)** DCB, **(b)** Toluene, **(c)** Chloroform, **(d)** THF, **(e)** Chlorobenzene and **(f)** Xylene solution.

**Figure 2:** Polarized optical microscopy micrographs of the surface of a P3HT:$C_{60}$ (1:1 wt. ratio) prepared from different solvents: (**a)** Toluene, **(b)** THF, **(c)** Xylene **(d)** CB (inset DCB) and **(e-h)** Chloroform. The images in **e**–**h** correspond to temperatures of 72, 170, 200 and 250 ºC, respectively. Note images in **a-d,** as well as the inset in **(e)** were taken at room temperature.

**Figure 3:** Diffraction patterns of (a) rr-P3HT and (b) P3HT:$C_{60}$ (1:1 wt. ratio) blend prepared from different solvents. The inset depicts the orientation of the P3HT crystalline domains with respect to the substrate (Fig 4a).

**Figure 4:** Raman spectrum of (a) P3HT film, as well as its blend, (b) 1:1 wt. ratio, prepared from different solvents and spin-coated on Si substrate.

**Figure 5:** FITR spectra of (a) P3HT film, as well as its blend, (b) 1:1 wt. ratio, prepared from different solvents and spin-coated on Si substrates.

**Figure 6:** UV-vis absorption spectra of **(a)** pure P3HT film, **(b)** P3HT:$C_{60}$ (1:1 wt. ratio) blend prepared from different solvents and spin-coated on ITO glass substrates.

**Figure 7:** Photoluminescence (PL) spectra of (a) P3HT film and (b) P3HT:$C_{60}$ blend film spin cast from different solvents on Si (100) substrates. Variation in intensity is observed for different solvents.

**Table1**: Boiling points of different solvents and their solubility in $C_{60}$ fullerene **[19, 20]**.

**Table 2:** Summary of the peak positions and grain sizes of the as-prepared P3HT films prepared from different solvents.

**Table 3:** Raman measurements of the C=C stretching deformations for the P3HT film and its blend (1:1 wt. ratio) prepared from different solvents and spin-coated on Si substrates.